

RESEARCH ARTICLE

# Investigating the effect of moisture protection on solid-state stability and dissolution of fenofibrate and ketoconazole solid dispersions using PXRD, HSDSC and Raman microscopy

Parijat Kanaujia<sup>1</sup>, Grace Lau<sup>1</sup>, Wai Kiong Ng<sup>1</sup>, Effendi Widjaja<sup>1</sup>, Martin Schreyer<sup>1</sup>, Andrea Hanefeld<sup>2</sup>, Matthias Fischbach<sup>2</sup>, Christoph Saal<sup>2</sup>, Mario Maio<sup>2</sup>, and Reginald B.H. Tan<sup>1,3</sup>

<sup>1</sup>*Institute of Chemical and Engineering Sciences, Jurong Island, Singapore*, <sup>2</sup>*Merck KGaA, Darmstadt, Germany*,

<sup>3</sup>*Department of Chemical and Biomolecular Engineering, The National University of Singapore, Singapore*

## Abstract

Enhanced dissolution of poorly soluble active pharmaceutical ingredients (APIs) in amorphous solid dispersions often diminishes during storage due to moisture-induced re-crystallization. This study aims to investigate the influence of moisture protection on solid-state stability and dissolution profiles of melt-extruded fenofibrate (FF) and ketoconazole (KC) solid dispersions. Samples were kept in open, closed and Activ-vials<sup>®</sup> to control the moisture uptake under accelerated conditions. During 13-week storage, changes in API crystallinity were quantified using powder X-ray diffraction (PXRD) (Rietveld analysis) and high sensitivity differential scanning calorimetry (HSDSC) and compared with any change in dissolution profiles. Trace crystallinity was observed by Raman microscopy, which otherwise was undetected by PXRD and HSDSC. Results showed that while moisture protection was ineffective in preventing the re-crystallization of amorphous FF, KC remained X-ray amorphous despite 5% moisture uptake. Regardless of the degree of crystallinity increase in FF, the enhanced dissolution properties were similarly diminished. Moisture uptake above 10% in KC samples also led to re-crystallization and significant decrease in dissolution rates. In conclusion, eliminating moisture sorption may not be sufficient in ensuring the stability of solid dispersions. Analytical quantification of API crystallinity is crucial in detecting subtle increase in crystallinity that can diminish the enhanced dissolution properties of solid dispersions.

**Keywords:** Melt extrusion, moisture protection, degree of crystallinity, stability studies, solid dispersion

## Introduction

In pharmaceutical research, the formulation of solid dispersions is generally accepted as a method to enhance the dissolution and oral bioavailability of drugs or new chemical entities (NCEs) with low aqueous solubility<sup>1</sup>. Despite the numerous publications on the development of solid dispersions, very few products based on this technology have been marketed primarily due to production and stability problems<sup>2,3</sup>. The use of industrially feasible methods like melt extrusion<sup>4,5</sup> and spray drying<sup>6</sup> for the manufacturing of solid dispersions has tackled scaling-up problems in production.

In a solid dispersion system, the active pharmaceutical ingredient (API) in amorphous form is dissolved or dispersed in the carrier matrix. The higher molecular mobility of amorphous materials may improve the solubility and dissolution rate of the API and, thus facilitate the gastrointestinal absorption of the active drugs<sup>7</sup>. However, the amorphous form tends to convert to the crystalline form upon aging due to its thermodynamic instability causing physical instability of the solid dispersions. The re-crystallization of API, which leads to a significant reduction in the dissolution rate during accelerated stability testing, is the major cause of failure in

*Address for Correspondence:* Parijat Kanaujia, Institute of Chemical and Engineering Sciences, 1 Pesek Road, Jurong Island, Singapore 627833. Tel.: +65 67963872; Fax: +65 63166183. E-mail: parijat\_kanaujia@ices.a-star.edu.sg; Reginald B. H. Tan, Institute of Chemical and Engineering Sciences, 1 Pesek Road, Jurong Island, Singapore 627833. Tel.: +6567963841; Fax: +65 63166183. E-mail: reginald\_tan@ices.a-star.edu.sg

(Received 04 October 2010; revised 12 January 2011; accepted 19 January 2011)

solid dispersion-based products<sup>8</sup>. The presence of moisture facilitates the re-crystallization process as water vapor is absorbed more easily by an amorphous solid<sup>9</sup>. Water acts as a plasticizer: it reduces glass transition temperature ( $T_g$ ) of the solid dispersion and increases the tendency to re-crystallize<sup>10</sup>. Some polymers have been reported to significantly delay the onset re-crystallization of APIs<sup>11–13</sup>. The effect of polymer type on the stabilization of indomethacin was reported<sup>14</sup>. Indomethacin was melt-extruded with Eudragit® EPO, polyvinylpyrrolidone (PVP) K30 and PVP-vinyl acetate at 30%, 50% and 70% drug loading. The Eudragit® EPO formulation at 30% drug level showed stabilization of the formulation from re-crystallization. The effect of surfactant on stability of melt-extruded polymer matrices of an API has been reported by Ghebremeskel<sup>15</sup>. The degree of crystallinity after stability studies was quantitatively determined by powder X-ray diffraction (PXRD). The surfactants acted as excellent plasticizer without affecting the stability of melt-extruded solid dispersion. The stabilization of solid dispersions depends upon many factors such as molecular mobility restriction of API, reduction in the driving force for crystallization, increase in the activation energy for crystallization, anti-nucleation effect, or a combination of these factors<sup>16</sup>. Recent reports have underscored the important effect of moisture sorption on the phase separation of amorphous API from polymeric excipients. Storage above 54% relative humidity was able to induce phase separation in PVP-based amorphous solid dispersions of nifedipine, droperidol and pimozone<sup>17</sup>. The polymer hygroscopicity is also an important factor which affects moisture-induced phase separation. The amorphous solid dispersions prepared from less hygroscopic polymers and having strong API-polymer interactions were less prone to phase separation upon storage<sup>18</sup>. Although moisture sorption plays an important role in the stability of solid dispersions, there is little literature on the effect of different levels of moisture sorption on the stability of solid dispersions during accelerated stress testing.

Therefore, the aim of this study was to investigate the use of moisture protection measures on the solid-state stability of melt-extruded solid dispersions together with any accompanying change in dissolution properties. Fenofibrate (FF) and ketoconazole (KC) were selected as model lipophilic APIs (Log *P*-values of 5.6 and 3.8, respectively) as they have significantly different glass transition temperatures: below and above room temperature (FF: –20°C and KC: 42°C). They are both reported to lack strong intermolecular interactions such as hydrogen bonding with polymers, which can contribute a stabilization effect. Kollidon® 17 PF (PVP) was selected as a highly hygroscopic polymer frequently used in melt extrusion to compare with the less moisture-sorption prone Kollidon® VA 64 (PVP copolymerized with polyvinyl acetate). Melt-extruded amorphous solid dispersions of FF and KC were stored at 40°C/75% RH for 13 weeks in open vials (free access to moisture),

closed vials (limited access to moisture) and Activ-vials® (no moisture) to study the effect of moisture protection on the re-crystallization of APIs. HSDSC and PXRD analyses were used to quantify the degree of crystallinity in the stability samples as an indicator of stability and the effect of API re-crystallization was compared with the measured dissolution profiles.

Various analytical techniques have been developed for the quantification of re-crystallization in amorphous solids<sup>19</sup>. The spectroscopic techniques like near infrared spectroscopy<sup>20</sup> and Raman spectroscopy<sup>21,22</sup> have been used in quantification of the degree of crystallinity. However, the pharmaceutical products generally contain several excipients along with API, and the interference caused by excipients makes the quantification of crystallinity difficult. The most common and definitive method of quantifying crystallinity is PXRD technique<sup>23</sup>. The lower limit of quantification of crystalline API in a predominantly amorphous system by PXRD is 5–10 wt.%<sup>24</sup>. However, this technique may not be suitable for solid dispersions where the crystallite size is very small which can induce peak broadening in the diffraction pattern<sup>25</sup>. HSDSC has been used to study the phase transformation, thermodynamic behavior and quantification of crystalline/amorphous content of pharmaceutical solids<sup>26</sup>. The lower limit of quantification of crystalline API in a largely amorphous system by HSDSC is 1–5 wt.%<sup>27</sup>. In this study, the results of PXRD (Rietveld analysis) and high sensitivity differential scanning calorimetry (HSDSC) in quantifying of the degree of crystallization in melt-extruded solid dispersions will be compared, which has not been reported in literature.

## Materials and methods

FF EP and KC BP were supplied by Smruthi Organics Ltd., India, and Piramal Healthcare Ltd., India, respectively. Kollidon® 17 PF (K17) and Kollidon® VA64 (KVA) were purchased from BASF, Germany. HPLC grade acetonitrile and methanol were supplied by Merck, Germany. Lecithin (Lipoid S 100) was purchased from Lipoid, Germany and other reagents were supplied by Sigma USA and used as supplied. Activ-vial® was supplied by CSP technologies, USA.

## Preparation of hot melt extrudates

The melting points of FF and KC are 82°C and 151°C, respectively while the  $T_g$  of K17 and KVA are 131°C and 101°C, respectively. In order to obtain clear transparent extrudates, the extrusion temperature was selected above the  $T_g$  of the polymers and melting temperature of the API. The FF samples were extruded at 135°C, whereas the KC samples were extruded at 165°C.

The physical mixtures of FF and KC (at 30 wt.%) and K17 (FF K17 PM and KC K17 PM) or KVA (FF KVA PM and KC KVA PM) were prepared by mixing in a turbula mixer (Willy A Bachofen, Basel Switzerland) for 15 min. The powder mixture was then manually fed into a preheated

melt extruder (HAAKE MiniLab II, Thermo Scientific, Germany). The speed of twin screw was fixed at 50 rpm and operated in flush mode. The extrudates were collected on a conveyor belt after air cooling and subsequently milled in a 50 ml stainless steel vessel using one stainless steel ball of 25 mm diameter (Retsch MM 200, Germany) for 2 min at 30 Hz frequency. The powdered solid dispersions were stored in screw-capped glass bottles in dry cabinet (15% RH) at room temperature for further use.

### Stability study

The stability study was performed according to the ICH Q 2 guideline for 13 weeks at 40°C/75% RH with sampling at 4, 8 and 13 weeks. Approximately 2.0 g of sample were placed in each glass vial. Glass vials were stored either uncapped (open vial) or capped (closed vial) inside the humidity chamber. In order to prevent the absorption of moisture by the samples during the storage, the Activ-vials® were used. The Activ-vial® consists of a flip-top closed vial with integrated molecular sieve sleeve to prevent moisture absorption. Separate vials were kept for analysis at every time point after weighing. After specific time intervals, the vials were removed, inspected visually for the physical appearance, weighed using an analytical balance (Sartorius AG, Germany) and characterized by PXRD, HSDSC and Raman microscopy. Beyond 4 weeks, only Activ-vial® samples were analyzed.

### PXRD

The crystallinity of API present in the different samples was determined by PXRD. The PXRD patterns of the physical mixtures and extruded samples were recorded on an X-ray powder diffractometer (D8 Advance, Bruker AXS GmbH, Germany) equipped with a PSD Vantec-1 detector. Measurements were performed with CuK $\alpha$  radiation over the angular range from  $4 < 2\theta < 50^\circ$  in step scan mode (step width  $0.02^\circ$ , scan rate  $1^\circ/\text{min}$ ).

Rietveld refinements were performed employing the fundamental parameter approach developed by Cheary and Coelho<sup>28</sup> as implemented in Topas 4.2 (Bruker AXS 2009). For FF, the structure published by Henry et al.<sup>29</sup> was used as a starting model and only scale factor, lattice parameters and an averaged isothermal parameter were refined and structure from Cambridge Structural Database System served as reference for KC. First, a pure phase powder X-ray diffractogram of API was refined, and it was found to be necessary to apply the March-Dollase correction<sup>30</sup> for preferred orientation in (1 -1 1) and (1 1 0) direction. The extruded mixtures, however, showed little or no preferred orientation. Subsequently, Rietveld refinements were performed on physical mixtures and extruded samples after 0, 4, 8 and 13 weeks of storage at 40°C and a relative humidity of 75%. The amorphous “humps” in these samples were fitted by adding up to three broad Split Pseudo Voigt peaks into the patterns and refining their peak shapes, positions and intensities. The scale factors of FF and KC for each refinement were

recorded, and the ones of the physical mixtures were normalized to 100%.

The objective of the Rietveld analysis was to determine how much of the originally weighed API re-crystallized after a given time. This was achieved by a variant of the external standard approach<sup>31</sup>. The relationship between the weight fraction of a substance  $w_s$ , the Rietveld scale factor  $S_s$ , for a given diffractometer configuration with diffractometer constant  $K$  is given by Equation 1 where  $(ZMV)_s$  is the mass volume product of substance  $s$  and  $\mu_{\text{mix}}$  is the X-ray mass absorption coefficient of the mixture of which  $s$  is one constituent.

$$w_s = \frac{S_s \times (ZMV)_s \times \mu_{\text{mix}}}{K} \quad (1)$$

The constancy of the diffractometer constant throughout the series of experiments was ensured by using the same conditions and control files for all experiments and confirmed by weekly measurements of the NIST corundum standard SRM1976<sup>32</sup>. The chemical compositions of all mixtures were identical as the ratio of API and the polymers were constant. Therefore all components in Equation 1 with the exception of the scale factor and the weight fraction remain constant for all experiments. A physical mixture of crystalline API and polymer was used for calibration and the degree of crystallinity ( $\chi$ ) can be calculated as:

$$\chi_{\text{recryst}} = \frac{S_{\text{recryst}}}{S_{\text{calibration}}} \times 100 \quad (2)$$

### HSDSC

HSDSC measurements were performed using Perkin Elmer Diamond DSC (Perkin Elmer USA). The enthalpic response was calibrated with Indium. The sample (~3.0 mg) was heated from 20°C to 200°C at  $10^\circ\text{C}/\text{min}$  in sealed aluminum pan. The data treatment and integration were done by Pyris Analysis (Perkin Elmer, USA). The degree of crystallinity ( $\chi$ ) of the solid dispersions was calculated from the calorimetric data<sup>33</sup> using following equation.

$$\chi_{\text{recryst}} = \frac{\Delta H_s}{\Delta H_c} \times 100 \quad (3)$$

where  $\Delta H_s$  is heat of fusion of solid dispersion sample and  $\Delta H_c$  is heat of fusion of the drug polymer physical mixture containing fully crystalline drug in the same weight ratio.

### Raman microscopy

Raman microscopy was used to detect any crystallinity in the amorphous solid dispersions qualitatively and obtain the spatial distribution of API in the polymer matrices. The Raman mapping measurements were performed using a Raman microscope (InVia Reflex, Renishaw UK) equipped with near infrared enhanced deep-depleted thermoelectrically Peltier cooled CCD



array detector (576×384 pixels) and a high grade Leica microscope. The sample was irradiated with a 785 nm near infrared diode laser (laser power 50–100 mW) and a 50× objective lens was used to collect the backscattered light. Raman point-by-point mapping with a step size of 2 µm in both the *x* and *y* directions was performed in an area of 40 µm × 40 µm. Measurement scans were collected using a static 1800 groove per mm dispersive grating in a spectral window from 700 to 1800 cm<sup>-1</sup>. Since the collected raw Raman spectra were combination of Raman scattering signals, spikes due to cosmic rays, and some autofluorescence background, spectral preprocessing was carried out in order to generate Raman spectral alone. Spikes were removed in the first step followed by baseline correction. The preprocessed Raman mapping data was then analyzed using the band-target entropy minimization (BTEM) algorithm to reconstruct the pure component spectra from the extruded samples<sup>34</sup>. BTEM algorithm is one of the self-modeling curve resolution (SMCR) techniques, which was developed to recover the pure component spectra of underlying constituents from a set of mixed spectra without recourse to any a priori known spectral libraries and has been proven well to reconstruct pure component spectra of minor components<sup>35,36</sup>.

### Dissolution testing

The dissolution of APIs, physical mixture of APIs with polymers and solid dispersions, was performed on 8-station paddle type dissolution apparatus II of USP (VK 7010 Varian Inc., Palo Alto, CA, USA). The test was performed at 37±0.5°C with paddle speed of 75 rpm using 500 ml of simulated gastric fluid (pH 1.2) containing 0.1% w/w Tween 80 and new FASSIF (pH 6.5) as dissolution media<sup>37</sup> for samples containing FF and KC, respectively. Powder containing approximately 100 mg of API was weighed and added to the 500 ml of dissolution media at 37±0.5°C. The samples were withdrawn at different time points, filtered through 0.22 µm syringe filter and analyzed by HPLC (Agilent HPLC 1100 series equipped with Agilent Quat pump and auto sampler).

## Results and discussion

### Stability study

All extrudates were clear, transparent and cylindrical in shape which suggests the formation of homogeneous solid dispersions. After milling, solid dispersions were converted to white, free flowing powders. The milled solid dispersions were stored in open, closed and Activ-vial® under 40°C/75% RH for the stability study. All Activ-vial® samples remained as free flowing powders after 13 weeks. In open vials, the solid dispersions containing K17 formed a soft sticky solid, whereas those with KVA became very hard solids. The closed vial samples remained largely in powder form with some agglomeration with the exception of FF K17 which formed a soft sticky cake. The weight gain due to moisture absorption is recorded in Table 1.

In open vials, the solid dispersions containing K17 absorbed substantial quantities of moisture at more than 20%, whereas KVA-based solid dispersions took in over 10%. The closed vials were able to significantly reduce the level of moisture sorption of FF KVA, KC K17 and KC KVA samples but not for FF K17. The Activ-vials® were equally effective in protecting all stability samples from moisture sorption.

### PXRD

Before milling, PXRD analysis of FF extruded with K17 (FF K17) showed a halo indicating the X-ray amorphous state as shown in Figure 1A h. Subsequent milling resulted in some re-crystallization as seen from the characteristic crystalline diffraction peaks of FF in Figure 1A b. The hygroscopic nature of K17, low molecular weight, low solubility of FF in K17 melt and milling process might have assisted in re-crystallization of FF from FF-K17. The peaks were identified as FF with the strongest intensities coinciding with the peaks found in the diffraction pattern of the physical mixture and also with FF pattern in the Cambridge structural database. The increase in peak heights of diffraction pattern of the FF K17 stored in open and closed vials for 4 weeks suggested faster re-crystallization of FF than those in Activ-vials® samples, which gave similar diffraction pattern as freshly milled sample after being stored for 4, 8 and 13 weeks (Figure 1A e, f and g).

After milling, the PXRD of FF KVA gave a characteristic amorphous halo indicating that the solid dispersion was amorphous (Figure 1B b). After 4 weeks of storage in closed and Activ-vials®, the characteristic diffraction peaks of crystalline FF appeared indicating the occurrence of re-crystallization. However, the diffractogram of the open vial sample gave a halo with emergence of one broad peak shifting to higher 2θ values (Figure 1B c). This was unexpected, inconsistent with HSDSC data as shown later and excluded from the analysis. PXRD of Activ-vials® samples after 8 and 13 weeks showed similar FF crystalline peaks as those after 4 weeks (Figure 1B e, f and g).

The PXRD patterns of KC K17 and KC KVA gave a characteristic amorphous halo after milling (Figure 2 b). After 4 weeks in open vials, characteristic diffraction peaks of KC appeared indicating re-crystallization of KC (Figure 2 c), whereas closed vial and Activ-vial® samples remained X-ray amorphous (Figure 2 d). After 8 and 13 weeks of storage in Activ-vials®, the PXRD pattern of KC K17 and KC KVA remained a halo confirming re-crystallization was inhibited (Figure 2 e, f and g).

Table 1. Weight gain by the stability samples at 40°C/75% RH.

Condition	%w/w weight increase			
	FF K17	FF KVA	KC K17	KC KVA
4 weeks in open vial	21.1	11.7	20.1	11.5
4 weeks in closed vial	16.7	2.9	5.7	4.8
4 weeks in Activ-vial®	0.0	0.0	0.0	0.0
8 weeks in Activ-vial®	0.0	0.0	0.0	0.0
13 weeks in Activ-vial®	0.0	0.0	0.0	0.0

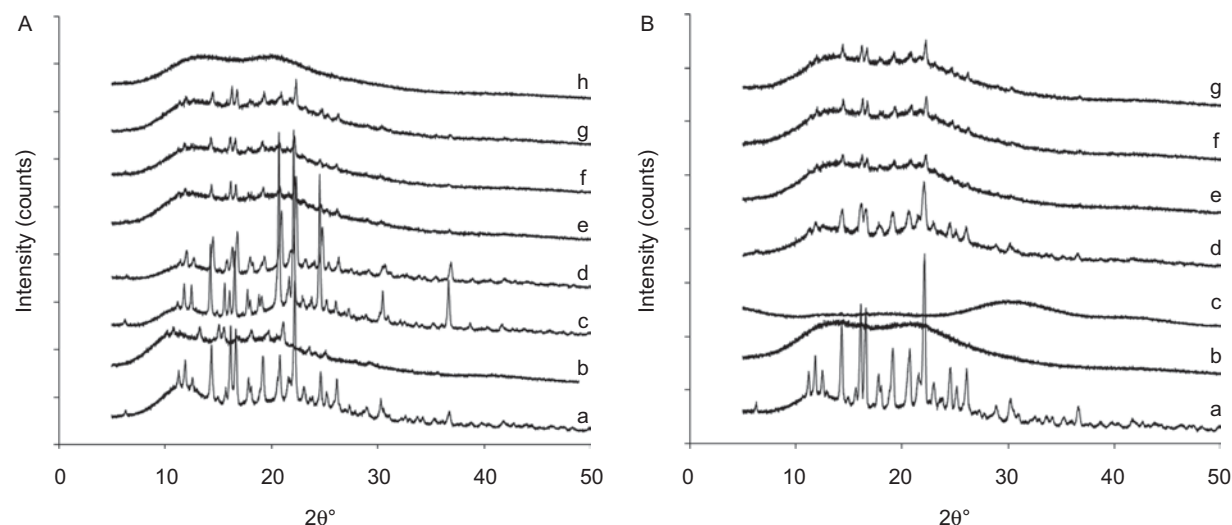


Figure 1. PXRD diffractogram of the FF K17 (A) and FF KVA (B) 0–13 week at 40°C/75% RH (a) physical mixture; (b) immediately after milling; (c) 4 weeks in open vial; (d) 4 weeks in closed vial; (e) 4 weeks in Activ-vial®; (f) 8 weeks in Activ-vial®; (g) 13 weeks in Activ-vial® and (h) FF K17 extruded unmilled.

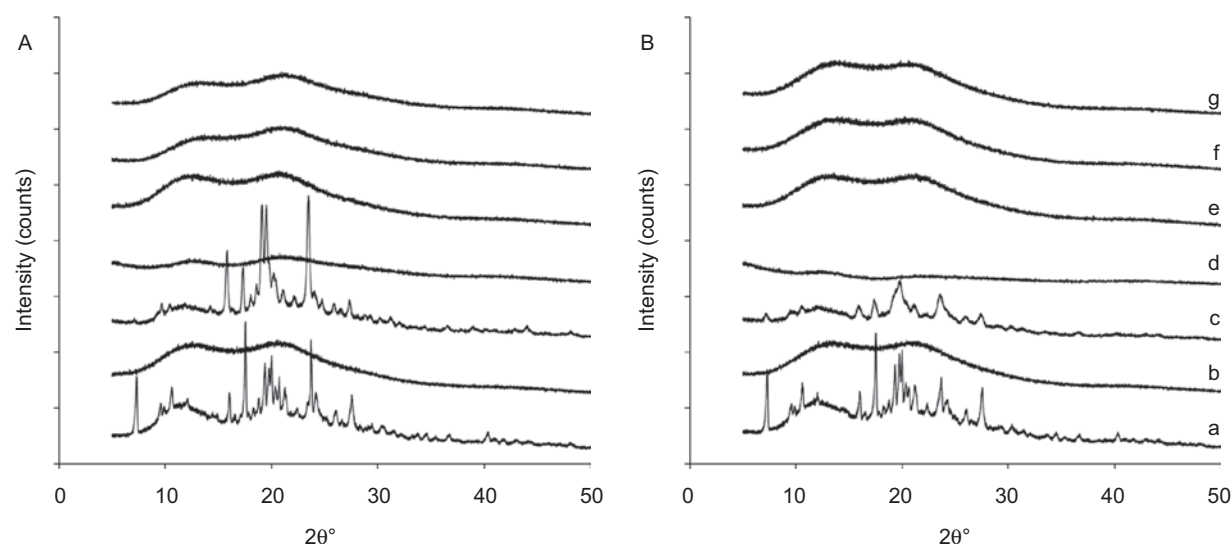


Figure 2. PXRD diffractogram of the KC K17 (A) and KC KVA (B) 0–13 week at 40°C/75% RH (a) physical mixture; (b) immediately after milling; (c) 4 weeks open vial; (d) 4 weeks closed vial; (e) 4 weeks Activ-vial®; (f) 8 weeks Activ-vial®; (g) 13 weeks Activ-vial®.

The degree of crystallinity of different samples was calculated using Equation 2. Figure 3 gives a typical Rietveld refinement and the decomposition of the powder pattern into background, amorphous scattering and Bragg diffraction of FF with K17. Figure 3(A) shows observed pattern of FF K17 physical mixture superimposed on calculated pattern, the difference plot and the background that is due to air scattering. Figure 3(B) shows the observed pattern, the difference plot and the intensities of the three broad amorphous peaks or humps. The area below these amorphous peaks is integrated. Figure 3(C) shows the observed pattern, the difference plot and the calculated diffraction pattern of FF (Bragg diffraction). The area of this diffraction pattern is integrated for analysis. The areas in Figure 3(B) and 3(C) are normalized to give 100% and the figure 3(C) gives the degree of crystallinity.

The degrees of crystallization calculated from Rietveld analysis are listed in Table 2. After 4 weeks, the FF K17 open and closed vial samples showed 23.4% and 18% crystallinity, respectively, whereas the crystalline amount of Activ-vial® sample was only 5.1%. The FF KVA closed vial sample showed 12% crystallinity after 4 weeks, whereas in the Activ-vial® sample, 3.6% FF has re-crystallized. The degree of crystallinity with respect to the total FF present was calculated by multiplying the figures by 0.3 as the FF content was 30 wt.%. With a low  $T_g$  of FF at  $-20^\circ\text{C}$ , the presence of a stabilizing polymer like K17 or KVA may be inadequate to inhibit the molecular mobility of FF at 40°C even with moisture protection.

In open vials, most of the amorphous KC has re-crystallized within 4 weeks after absorbing 20.1% and 11.5% moisture in KC K17 and KC KVA, respectively. Despite 5.7% and 4.8% moisture uptake in KC K17 and KC KVA

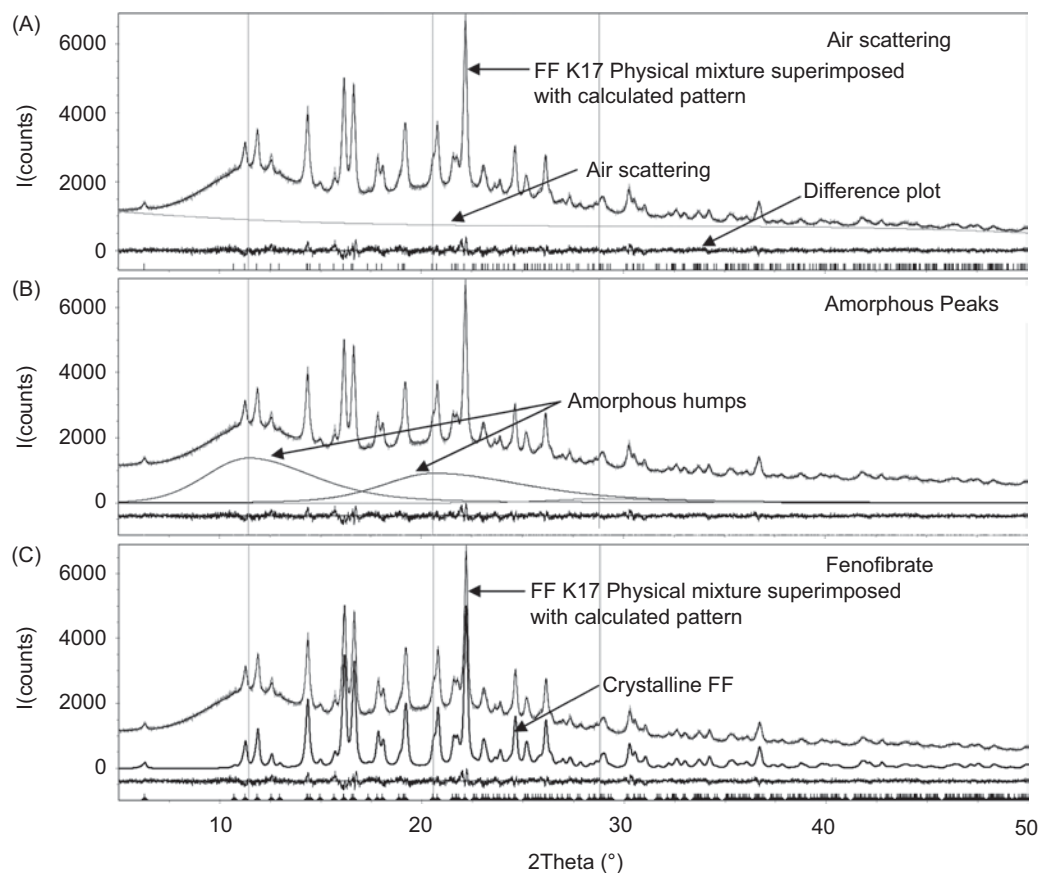


Figure 3. Rietveld refinement and the decomposition of the powder pattern into (A) diffuse air scattering, (B) amorphous humps and (C) Bragg diffraction of crystalline fenofibrate.

Table 2. Degrees of crystallinity calculated using Rietveld analysis of PXRD data.

Condition	Degree of crystallinity (%)			
	FF K17	FF KVA	KC K17	KC KVA
Physical mixture	30	—	—	—
Before storage	1.8	0.0	0.0	0.0
4 weeks open vial	23.4	Excluded	27.4	26.6
4 weeks closed vial	18	12	0.0	0.0
4 weeks Activ-vial®	5.1	3.6	0.0	0.0
8 weeks Activ-vial®	5.8	4.1	0.0	0.0
13 weeks Activ-vial®	6.2	4.6	0.0	0.0

in closed vial, there was no indication of crystallinity. This could be explained by the relatively high  $T_g$  of KC at 42.1°C, whereby storage temperature below  $T_g$  may not provide to sufficient molecular mobility for KC molecules to re-crystallize in the presence of stabilizing polymers like K17 and KVA.

### HSDSC

The enthalpy of fusion and calculated degrees of crystallinity from HSDSC data of FF samples are given in Table 3. The physical mixture of 30 wt.% crystalline FF with polymer was used as reference in order to nullify the effect of polymer. The amorphous FF present in open and closed vial samples re-crystallized after absorbing moisture as shown by HSDSC data. The higher than 30%

crystallinity for FF K17 samples may be due to separation of FF from polymeric matrix upon moisture absorption (<20 wt.%) and formation of crystalline FF rich zones and polymer-rich zones causing inhomogeneity as reported in the case of solid dispersions of PVP with nifedipine, droperidol and pimozide where the solid dispersions formed drug-rich and polymer-rich phases which led to the re-crystallization of drug upon storage at high humidity<sup>17,18</sup>. The FF K17 sample in Activ-vial® showed that almost a quarter of FF has been re-crystallized after 4 weeks which remained fairly unchanged after 8 and 13 weeks. The FF KVA samples in Activ-vial® showed 3.9% crystallinity after 4 weeks which increased to 5.3% and 5.5% after 8 and 13 weeks, respectively.

The different degrees of FF crystallinity in Activ-vial® between FF K17 and FF KVA samples were probably due to the different stabilizing effect of K17 and KVA as there was no moisture sorption in both cases. From PXRD and HSDSC analyses of FF samples, it is clear that the difference in crystallinity between open, closed and Activ-vial® samples were due to the different levels of moisture protection, which are consistent with moisture sorption data in Table 1. The degree of crystallization calculated from PXRD data and HSDSC data revealed that both methods are comparable when the moisture content is low, e.g., samples of milled FF K17 before storage, Activ-vial® samples of FF K17 and FF KVA. The absence of

moisture sorption in the Activ-vial® could not prevent the re-crystallization of FF, but the rate of re-crystallization was reduced significantly.

The HSDSC thermogram of physical mixture containing KC and K17 or KVA did not reveal any distinct melting endotherm of KC as it may be solubilized into the polymer upon heating. KC K17 and KC KVA formulations also did not give melting endotherm of KC after stability studies. Similar observations were reported by Mididoddi et al.<sup>38</sup> when KC was extruded with polyethylene oxide.

### Raman microscopy

The Raman microscopy was used to evaluate the presence of any trace crystallinity in samples before and after stability tests. Trace crystallinity was detected in FF K17 prior to stability tests and BTEM analysis could recover the pure component spectrum of crystalline form of FF. The presence of crystalline phase was similarly observed by PXRD (Figure 1A b) and HSDSC (Table 3). In FF KVA sample, trace crystallinity of FF was picked up from Raman microscopy although the pure component spectrum of crystalline FF could not be separated from

Table 3. Heat of fusion and degree of crystallinity calculated from HSDSC for FF K17 and FF KVA stability samples stored at 40°C/75% RH.

Condition	Degree of crystallinity (%)		Heat of fusion (J/g)	
	FF K17	FF KVA	FF K17	FF KVA
Physical mixture	30	30	18.10	23.18
Before storage	2.1	0.0	1.3	—
4 weeks open vial	38.6	25.2	22.6	19.4
4 weeks closed vial	38.6	21.6	22.6	16.7
4 weeks Activ-vial®	8.04	3.9	4.8	3.0
8 weeks Activ-vial®	9.1	5.3	5.5	4.1
13 weeks Activ-vial®	8.9	5.5	5.4	4.3

the spectra of FF and KVA by BTEM analysis (Figure 4A). This was likely due to the homogeneous distribution between FF and KVA as shown in the well distributed color mapping in Figure 4A. In contrast to FF K17, PXRD (Figure 1B b) and HSDSC were unable to detect any crystallinity in FF KVA.

After 13 weeks of storage in Activ-vial® at 40°C/75%RH, BTEM analysis could recover pure component spectra of amorphous and crystalline FF and KVA indicating the separation of both components under stressed conditions. The relative intensity of crystalline FF increased with a reduction in the intensity of amorphous FF after 13 weeks storage at 40°C/75%RH (Figure 4B). With a higher degree of crystallinity, this was also seen in PXRD (Figure 1B g) and HSDSC analyses (Table 3).

In KC solid dispersions, the results of Raman microscopy were in agreement with PXRD data except in KC K17 sample after 13 weeks in Activ-vial®. While the PXRD diffractogram described an amorphous halo, Raman microscopy showed traces of crystalline KC as shown in Figure 5B. However, as BTEM analysis could not separate the pure component spectra of KC and K17, the two components have remained homogeneously distributed after 13 weeks of stability testing (Figure 5A and 5B).

The detection of trace crystallinity by Raman microscopy, which was not shown by PXRD or HSDSC, was likely due to the low level of crystallinity below the detection limits of PXRD and HSDSC. The crystallite size could also be so small that particle induced line broadening distorted the PXRD pattern<sup>25</sup>.

### Dissolution testing

The primary objective of preparing solid dispersions is to enhance the dissolution rate of poorly soluble drugs by stabilizing them in the meta-stable amorphous state. The dissolution of the physical mixture

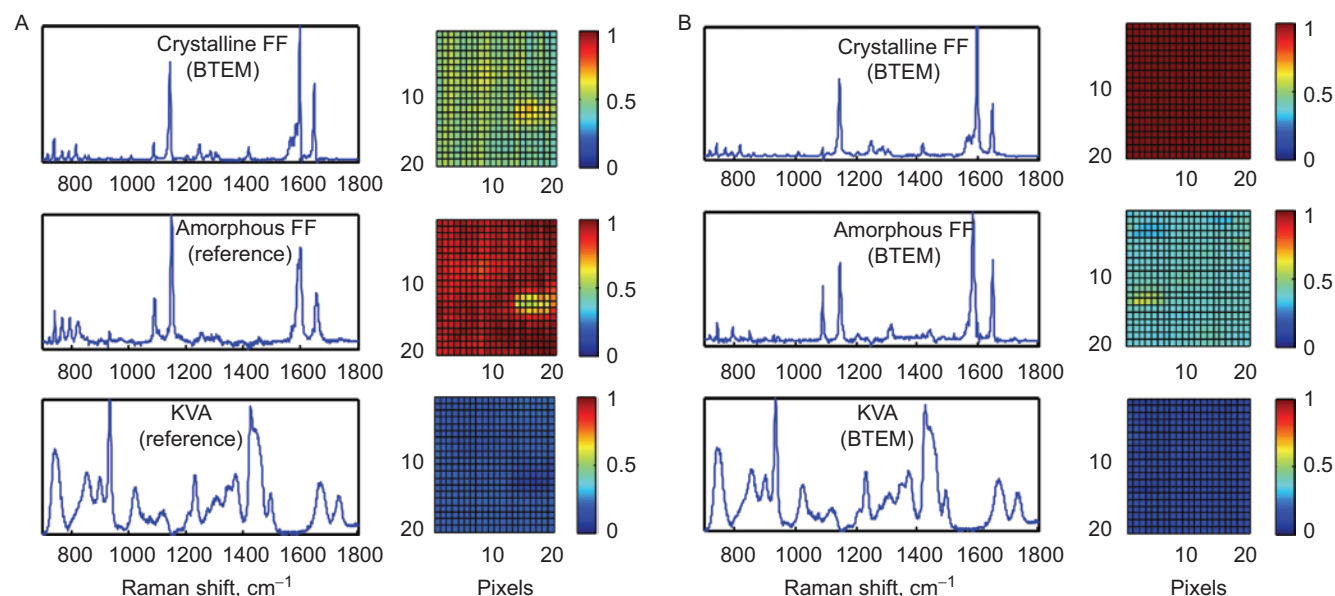


Figure 4. Raman microscopy of FF KVA at initial (A) and after 13 weeks storage in Activ-vial® at 40°C/75% RH (B) (The axes of score images are in pixels and can be directly correlated to distance by multiplying each pixel with 2 µm).



containing crystalline FF progressed very slowly at only 4% dissolution after 120 min; whereas, extruded FF K17 and FF KVA attained the plateau concentration in the initial 10–20 min of testing showing significantly higher dissolution rates and remained constant for 2 h of testing period. The absence of precipitation phase after the initial solubilization phase in the dissolution profile could be due to micellar solubilization of FF as the dissolution media contains 0.1% w/w Tween 80<sup>39</sup>. After storage at 40°C/75% RH in open, closed and Activ-vials® for 4 weeks, the dissolution rates of both FF K17 and FF KVA reduced significantly to the level of physical mixture. Dissolution remained at the same level for Activ-vial® samples after 8 and 13 weeks (Figure 6A and 6B), although only 5–6% of FF was re-crystallized upon storage. The reduction in dissolution rate could be attributed to the re-crystallization of the FF after storage as shown by the HSDSC, PXRD and Raman microscopy data. The separation of FF from the polymer matrix under Raman microscopy and re-crystallization may

also have reduced wetting of the solid dispersion particles to decrease the dissolution rate.

The physical mixture of KC with K17 and KVA gave 10.7% and 6.3% dissolution after 2 h, respectively; whereas, freshly extruded and milled KC K17 gave 39.8% dissolution and KC KVA gave 23.4% dissolution in FASSIF new pH 6.5 (Figure 7A and 7B). The crystalline KC alone showed 4.7% dissolution after 2 h in FASSIF new pH 6.5. After 4 weeks of storage at 40°C/75%RH, the dissolution rate of open vial samples was reduced significantly. The re-crystallization of the amorphous KC after moisture sorption as shown by the PXRD analysis is likely the major cause of the reduced dissolution. The solid dispersions stored in closed and Activ-vials® were able to retain high dissolution rates after 4 weeks of storage at 40°C/75% RH (Figure 7A and 7B). Enhanced dissolution properties of KC K17 and KC KVA in Activ-vials® were well retained after 13 weeks.

The dissolution of KC solid dispersions showed an initial burst release of 45–65% in first 10 min of the

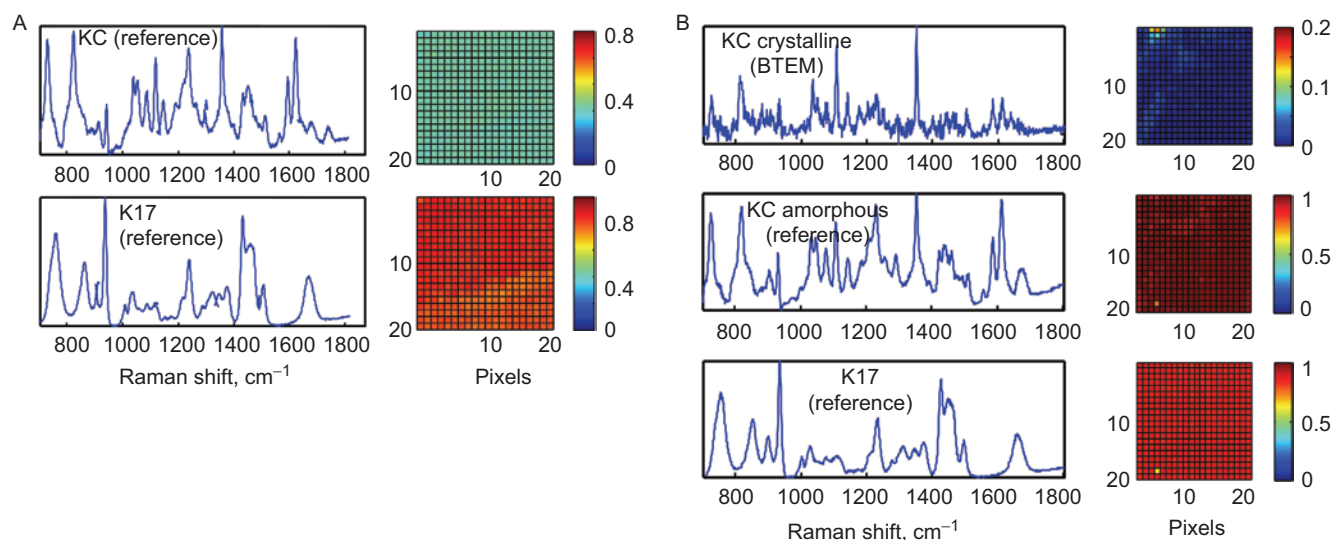


Figure 5. Raman microscopy of KC K17 at initial (A) and after 13 weeks storage in Activ-vial® at 40°C/75% RH (B) (The axes of score images are in pixels and can be directly correlated to distance by multiplying each pixel with 2 µm).

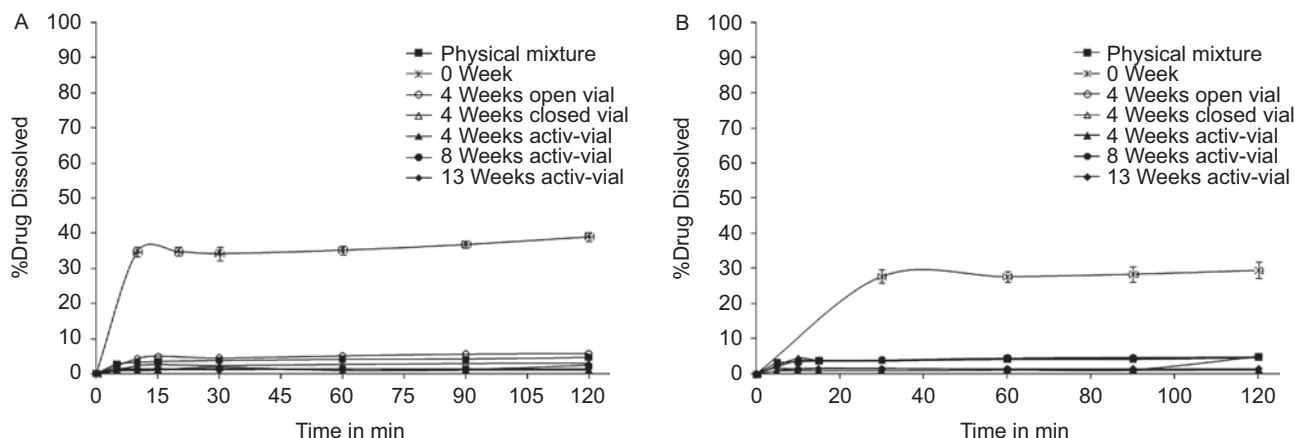


Figure 6. Dissolution profile of (A) FF K17 solid dispersion and (B) FF KVA solid dispersion stored at 40°C/75% RH in comparison with initial sample and physical mixtures.



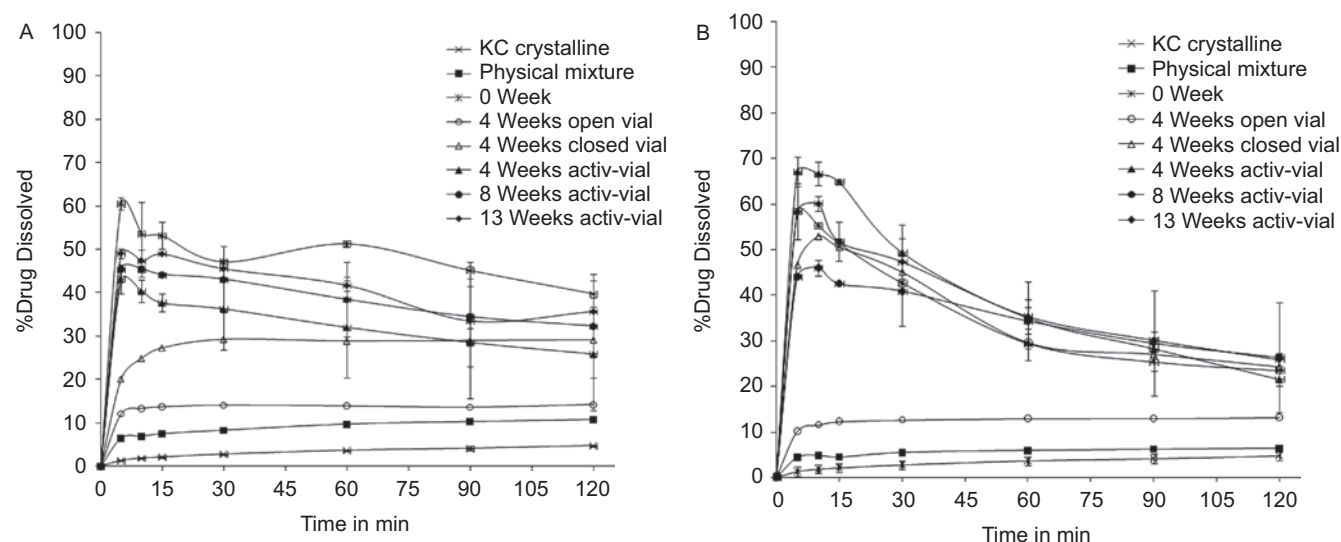


Figure 7. Dissolution profile of (A) KC K17 solid dispersion and (B) KC KVA solid dispersion stored at 40°C/75% RH in comparison with initial sample and KC physical mixtures.

dissolution followed by a sudden decrease in the dissolution rate. This may be attributed to the formation of supersaturated solution of KC in the dissolution media initially followed by the precipitation of the KC causing decrease in dissolution rate. The dissolution profiles of stressed samples of FF and KC are in complete agreement with re-crystallization occurrences as shown by PXRD, HSDSC and Raman microscopy.

## Discussion

The study shows that moisture protection using closed and Activ-vials® under accelerated stability conditions of 40°C and 75% RH was effective in stabilizing the amorphous state of solid dispersions of KC ( $T_g$  42°C) with K17 or KVA as well as retaining the enhanced dissolution properties. In closed vials, they were resistant to re-crystallization even after absorbing 5 wt.% moisture. In contrast, with a low  $T_g$  of -20°C, re-crystallization of FF solid dispersions occurs with or without any moisture sorption. The prevention of moisture sorption in FF solid dispersions using Activ-vials® could only slow down the rate of re-crystallization but does not prevent the loss in enhanced dissolution. Without moisture protection, both FF and KC solid dispersions re-crystallize in open vials. The loss in dissolution enhancement is likely due to phase separation from polymers and re-crystallization during stability testing.

The results of PXRD and HSDSC analyses were relatively comparable in quantifying the re-crystallization of FF during stability testing at low moisture contents (Activ-vial® samples). The PXRD analysis can be applied for both FF and KC solid dispersions while HSDSC was not suitable for KC as the API was solubilized in both K17 and KVA. Both PXRD and HSDSC analyses were found to be less sensitive to low traces of crystallinity as compared to Raman microscopy.

## Conclusion

Moisture plays an important role in the stability of solid dispersion but moisture protection alone was not effective in preventing the re-crystallization of FF due to its low  $T_g$ . As a small increase in API crystallinity may result in a complete loss of dissolution enhancement, quantification of low levels of crystalline content using PXRD and HSDSC may serve as a critical stability indicator for the performance of amorphous pharmaceutical formulations.

## Declaration of interest

The work was supported by the Science and Engineering Research Council (SERC) of A\* STAR (Agency for Science Technology and Research) Singapore.

## References

1. Vasanthavada M, Tong W, Serajuddin ATM. (2008). Development of solid dispersion for poorly water-soluble drugs. In: Liu R, ed. Water-insoluble drug formulation. Boca Raton: CRC Press, pp. 499-529.
2. Karanth H, Shenoy VS, Murthy RR. (2006). Industrially feasible alternative approaches in the manufacture of solid dispersions: a technical report. AAPS PharmSciTech, 7:87.
3. Repka MA, Majumdar S, Kumar Battu S, Srirangam R, Upadhye SB. (2008). Applications of hot-melt extrusion for drug delivery. Expert Opin Drug Deliv, 5:1357-1376.
4. Breitenbach J. (2002). Melt extrusion: from process to drug delivery technology. Eur J Pharm Biopharm, 54:107-117.
5. Repka MA, Battu SK, Upadhye SB, Thumma S, Crowley MM, Zhang F et al. (2007). Pharmaceutical applications of hot-melt extrusion: Part II. Drug Dev Ind Pharm, 33:1043-1057.
6. Friesen DT, Shanker R, Crew M, Smithey DT, Curatolo WJ, Nightingale JA. (2008). Hydroxypropyl methylcellulose acetate succinate-based spray-dried dispersions: an overview. Mol Pharm, 5:1003-1019.
7. Heinz A, Gordon KC, McGoverin CM, Rades T, Strachan CJ. (2009). Understanding the solid-state forms of fenofibrate-a

- spectroscopic and computational study. *Eur J Pharm Biopharm*, 71:100–108.
8. Serajuddin AT. (1999). Solid dispersion of poorly water-soluble drugs: early promises, subsequent problems, and recent breakthroughs. *J Pharm Sci*, 88:1058–1066.
  9. Saleki-Gerhardt A, Ahlneck C, Zografi G. (1994). Assessment of disorder in crystalline solids. *Int J Pharm*, 101:237–247.
  10. Ahlneck C, Zografi G. (1995). The molecular basis of moisture effects on the physical and chemical stability of drugs in the solid state. *Int J Pharm*, 123:265–271.
  11. Albers J, Alles R, Matthée K, Knop K, Nahrup JS, Kleinebudde P. (2009). Mechanism of drug release from polymethacrylate-based extrudates and milled strands prepared by hot-melt extrusion. *Eur J Pharm Biopharm*, 71:387–394.
  12. Hulsman S, Backensfeld T, Bodmeier R. (2001). Stability of extruded 17 $\beta$ -estradiol solid dispersions. *Pharma Dev Tech*, 6:223–229.
  13. Marsac PJ, Konno H, Rumondor ACF, Taylor LS. (2008). Re-crystallization of nifedipine and felodipine from amorphous molecular level solid dispersions containing poly(vinylpyrrolidone) and sorbed water. *Pharm Res*, 25:647–656.
  14. Chokshi RJ, Shah NH, Sandhu HK, Malick AW, Zia H. (2008). Stabilization of low glass transition temperature indomethacin formulations: impact of polymer-type and its concentration. *J Pharm Sci*, 97:2286–2298.
  15. Ghebremeskel AN, Vemavarapu C, Lodaya M. (2006). Use of surfactants as plasticizers in preparing solid dispersions of poorly soluble API: stability testing of selected solid dispersions. *Pharm Res*, 23:1928–1936.
  16. Bhugra C, Pikal MJ. (2008). Role of thermodynamic, molecular, and kinetic factors in crystallization from the amorphous state. *J Pharm Sci*, 97:1329–1349.
  17. Rumondor AC, Marsac PJ, Stanford LA, Taylor LS. (2009). Phase behavior of poly(vinylpyrrolidone) containing amorphous solid dispersions in the presence of moisture. *Mol Pharm*, 6:1492–1505.
  18. Rumondor ACF, Taylor LS. (2010). Effect of hygroscopicity on the phase behavior of amorphous solid dispersions in the presence of moisture. *Mol Pharm*, 7:477–490.
  19. Shah B, Kakumanu VK, Bansal AK. (2006). Analytical techniques for quantification of amorphous/crystalline phases in pharmaceutical solids. *J Pharm Sci*, 95:1641–1665.
  20. Bai SJ, Rani M, Suryanarayanan R, Carpenter JF, Nayar R, Manning MC. (2004). Quantification of glycine crystallinity by near-infrared (NIR) spectroscopy. *J Pharm Sci*, 93:2439–2447.
  21. Findlay WP, Bugay DE. (1998). Utilization of Fourier transform-Raman spectroscopy for the study of pharmaceutical crystal forms. *J Pharm Biomed Anal*, 16:921–930.
  22. Taylor LS, Zografi G. (1998). The quantitative analysis of crystallinity using FT-Raman spectroscopy. *Pharm Res*, 15:755–761.
  23. Yoshioka M, Hancock BC, Zografi G. (1994). Crystallization of indomethacin from the amorphous state below and above its glass transition temperature. *J Pharm Sci*, 83:1700–1705.
  24. Hancock BC, Zografi G. (1997). Characteristics and significance of the amorphous state in pharmaceutical systems. *J Pharm Sci*, 86:1–12.
  25. Suryanarayan R. (1995). X-ray powder diffractometry. In: Brittain HG, ed. *Physical characterization of pharmaceutical solids*. New York: Marcel Dekker, pp. 187–221.
  26. Vitez IM. (2004). Utilization of DSC for pharmaceutical crystal form quantitation. *J Therm Anal Calorim*, 78:33–45.
  27. Nagapudi K, Jona J. (2008). Amorphous active pharmaceutical ingredients in preclinical studies: preparation, characterization and formulation. *Curr Bioact Compd*, 4:213–224.
  28. Cheary RW, Coelho AA. (1992). A fundamental parameters approach to X-ray line-profile fitting. *J Appl Crystallogr*, 25:109–121.
  29. Henry RE, Zhang GZ, Gao Y. (2003). Fenofibrate. *Acta Cryst*, E59:O699–O700.
  30. Dollase WA. (1988). Correction of intensities for preferred orientation in powder diffractometry: application of the March model. *J Appl Crystallogr*, 21:86–91.
  31. Von Dreele RB. (2008). Rietveld refinement. In: Dinnebier RE, Billinge SJL, eds. *Powder Diffraction: Theory and practice*. Cambridge: RSC Publishing, pp. 266–279.
  32. Kaiser DL, Watters RL. (2007). Certificate of Analysis; Standard Reference Material 1976, National Institute of Standards, Gaithersburg, MD 20899, USA.
  33. Song J, Ren M, Chen Q, Wang S, Zhao Q, Zhang H, Mo Z. (2004). Determination of degree of crystallinity of nylon 1212 by wide-angle X-ray diffraction. *Ch J Poly Sci*, 22:491–496.
  34. Widjaja E, Li CZ, Chew W, Garland M. (2003). Band Target Entropy Minimization. A general and robust algorithm for pure component spectral recovery: application to complex randomized mixtures of six components. *Anal Chem*, 75:4499–4507.
  35. Breitenbach J, Schrof W, Neumann J. (1999). Confocal Raman spectroscopy: analytical approach to solid dispersions and mapping of drugs. *Pharm Res*, 16:1109–1113.
  36. Widjaja E, Seah RK. (2008). Application of Raman microscopy and band-target entropy minimization to identify minor components in model pharmaceutical tablets. *J Pharm Biomed Anal*, 46:274–281.
  37. Jantrati E, Janssen N, Reppas C, Dressman JB. (2008). Dissolution media simulating conditions in the proximal human gastrointestinal tract: an update. *Pharm Res*, 25:1663–1676.
  38. Mididoddi PK, Repka MA. (2007). Characterization of hot-melt extruded drug delivery systems for onychomycosis. *Eur J Pharm Biopharm*, 66:95–105.
  39. He H, Yang R, Tang X. (2010). *In vitro* and *in vivo* evaluation of fenofibrate solid dispersion prepared by hot-melt extrusion. *Drug Dev Ind Pharm*, 36:681–687.